

Velocity selection in the symmetric model of dendritic crystal growth

Angelo Barbieri, Daniel C. Hong, and J. S. Langer

Institute for Theoretical Physics, University of California, Santa Barbara, California 93106

(Received 8 July 1986)

We present an analytic solution of the problem of velocity selection in a fully nonlocal model of dendritic crystal growth. Our analysis uses a WKB technique to derive and evaluate a solvability condition for the existence of steady-state needlelike solidification fronts in the limit of small undercooling Δ . For the two-dimensional symmetric model with a capillary anisotropy of strength α , we find that the velocity is proportional to $\Delta^4 \alpha^{7/4}$. We also describe the application of our method in three dimensions.

I. INTRODUCTION

Developments reported recently by a number of investigators¹⁻³ point to the emergence of an exact analytic theory of velocity selection in realistic, fully nonlocal models of dendritic crystal growth.⁴ Such a theory may have important implications for understanding mechanisms of pattern formation in a variety of other physical situations; indeed, the present developments have occurred in parallel with closely related work on the viscous fingering problem of Saffman and Taylor.⁵⁻⁸ In what follows, we shall describe some recent calculations pertaining to needle crystals in both the two- and three-dimensional symmetric models of solidification for the experimentally relevant limit of low undercooling. In addition to recovering features of this model that have appeared in recent numerical investigations,^{9,10} we are able to obtain an explicit relation between the selected velocity and the strength of the anisotropy in two dimensions. Our results in three dimensions are less complete at present but do confirm the general structure of the theory and provide some interesting new mathematical insights.

The conceptual basis for the work to be described here is the discovery, initially in connection with simplified local models,^{11,12} that surface tension is a singular perturbation which leads to a nontrivial solvability condition for needlelike steady-state solutions of the equations of motion for crystal growth, and that this solvability condition identifies the dynamically selected state of the system. For the realistic nonlocal model to be discussed here, the appropriately scaled form for the solvability condition was first pointed out by Pelcé and Pomeau.² A second stage in these developments has been the discovery of a mathematical strategy that enables us to make asymptotically accurate estimates of the singular effects of the capillary perturbation. A linear analysis of two local models, making essential use of WKB methods, was presented by one of us (J.S.L.) along with numerical evi-

dence for its validity.^{13,14} In an as yet unpublished investigation, Kruskal and Segur¹⁵ have found an elegant way of understanding why the linearization suggested in Ref. 13 succeeds in capturing the essential features of the underlying nonlinear problem. The method of Kruskal and Segur has been applied directly by Pomeau and co-workers to both the Saffman-Taylor problem⁷ and the two-dimensional needle crystal to be discussed here.³

The crucial step in both the linear theory and also at a deeper point on the Kruskal-Segur analysis is the derivation of an inhomogeneous linear equation for the capillary correction to the shape of the needle crystal. In our earlier work on the local models,^{13,14} we were able to use the WKB method to construct an explicit solution to this equation which could then be matched to appropriate boundary conditions in order to deduce the solvability condition. It was pointed out in Ref. 13 that the solvability condition deduced by direct geometrical considerations is formally identical to the mathematically more conventional notion of solvability in situations of this kind: that the inhomogeneous term must be orthogonal to the null space of the linear operator. Shraiman, in his work on the Saffman-Taylor problem,⁶ has argued that the latter interpretation is apt to be more powerful because it may be applied in situations where explicit solutions are difficult or even intrinsically impossible to obtain. We shall adopt Shraiman's point of view here.

II. TWO DIMENSIONS

The steady-state equation of motion for the two-dimensional symmetric model⁴ is conveniently expressed in the form

$$\Delta - \frac{d_0}{\rho} \mathcal{K}_2\{\xi(x)\} = p \Gamma_2\{p, x, \xi(x)\}, \quad (2.1)$$

where

$$\Gamma_2(p, x, \xi(x)) = \int_0^\infty \frac{d\tau}{2\pi\tau} \int_{-\infty}^\infty dx' \exp \left\{ -\frac{p}{2\tau} \{(x-x')^2 + [\xi(x) - \xi(x') + \tau]^2\} \right\}. \quad (2.2)$$

Here $\zeta(x)$ identifies the solidification front which we may imagine to be nearly but not quite an Ivantsov¹⁶ parabola,

$$\zeta_{\text{Iv}}(x) = -\frac{x^2}{2}, \quad (2.3)$$

advancing at constant speed in the direction of its axis of symmetry. All lengths are measured in units of ρ , the (dimensional) radius of curvature at the Ivantsov tip. The left-hand side of (2.1) is a dimensionless expression for the temperature along the front as determined by thermodynamic equilibrium. More precisely, this quantity is $(T - T_\infty)/(L/c)$, where T_∞ is the temperature infinitely far away in the fluid, L is the latent heat, and c is the specific heat. Δ is the dimensionless undercooling $(T_M - T_\infty)/(L/c)$, where T_M is the melting temperature. The Gibbs-Thomson correction $d_0 \mathcal{K}_2/\rho$ contains the capillary length $d_0 = \gamma T_M c/L^2$, where γ is the surface tension, and is proportional to the two-dimensional curvature:

$$\mathcal{K}_2\{\zeta(x)\} = -\frac{\frac{d^2\zeta}{dx^2}}{\left[1 + \left(\frac{d\zeta}{dx}\right)^2\right]^{3/2}}. \quad (2.4)$$

Crystalline anisotropy enters via d_0 , which we shall assume to have the form $\bar{d}_0 A(\eta)$, where $\eta = \tan\theta = d\zeta/dx$, and

$$A(\eta) = 1 - \alpha \cos(4\theta) = 1 - \alpha + \frac{8\alpha\eta^2}{(1+\eta^2)^2} \quad (2.5)$$

for fourfold symmetry.

The right-hand side of (2.1) is this same dimensionless temperature determined by solving the diffusion problem with the understanding that, in the symmetric model where the diffusion constant D is the same in both phases, the solidification front acts simply as a line source of latent heat moving at constant speed. The reader should recognize that the integrand in Γ_2 is the Green's function for diffusion in a moving frame. The parameter $p = v\rho/2D$ is the thermal Péclet number; and v is the growth velocity that is ultimately to be determined by this calculation.

In the absence of surface tension, $d_0 = 0$, the Ivantsov parabola is an exact solution of (2.1) that we can take to define Δ as a function of p :

$$\begin{aligned} \Delta(p) &= p \Gamma_2\{p, x, \zeta_{\text{Iv}}(x)\} \\ &= 2\sqrt{p} e^p \int_{p^{1/2}}^{\infty} e^{-y^2} dy \approx (\pi p)^{1/2}, \end{aligned} \quad (2.6)$$

where the last approximation is valid for small p . We shall be interested in small values of the undercooling, $\Delta \ll 1$, which means $p \ll 1$ in (2.6). Note that this is the extreme nonlocal limit of the problem in which the tip radius ρ is much smaller than the range of the diffusion field $2D/v$. Values of p , for example, in Glickman's¹⁷ classic measurements of dendritic growth rates and morphologies in succinonitrile were of order 10^{-1} or 10^{-2} . Notice also that it is not until we have written (2.6) that we actually have defined the length scale ρ as the Ivantsov radius associated with initially prescribed values of Δ and v . The actual tip radius for nonzero values of d_0 is $\rho \mathcal{K}_2^{-1}(\theta=0)$, which may be near but not exactly equal to ρ .

Pelce and Pomeau² have shown how to derive the Ivantsov result (2.6) by direct evaluation of $\Gamma_2\{p, x, \zeta_{\text{Iv}}(x)\}$. They also point out that, because \mathcal{K}_2 must vanish at large $|x|$ for an acceptable needle crystal even with nonzero d_0 , it makes sense to subtract (2.6) from (2.1), thereby obtaining an integro-differential equation for $\zeta(x)$. In our notation, this equation is

$$-\sigma \mathcal{K}_2\{\zeta(x)\} = \Gamma_2\{p, x, \zeta(x)\} - \Gamma_2\{p, x, \zeta_{\text{Iv}}(x)\}, \quad (2.7)$$

where

$$\sigma = \frac{d_0}{p\rho} = \frac{2d_0D}{v\rho^2} \quad (2.8)$$

is the same dimensionless group of parameters that appeared in the marginal-stability theory.¹⁸ The fact that σ appears in (2.7) as the coefficient of the highest derivatives in the equation, plus the fact that, once the subtraction is made, the nonlinear integral operator on the right-hand side of (2.7) is well behaved in the limit $p \rightarrow 0$, implies that physically acceptable solutions are likely to exist only for special values of σ . In other words, (2.7) is a nonlinear eigenvalue equation which determines a selection rule of the form $\sigma = \sigma^*(\alpha, p)$, where σ^* has a definite value in the limit $p \rightarrow 0$.

To compute σ^* explicitly, we linearize (2.7) in the difference

$$\zeta_1(x) = \zeta(x) - \zeta_{\text{Iv}}(x). \quad (2.9)$$

The result is an inhomogeneous linear equation for ζ_1 which, in the limit of small p , becomes

$$\sigma \frac{d^2\zeta_1}{dx^2} - \frac{3\sigma x}{1+x^2} \frac{d\zeta_1}{dx} - \frac{(1+x^2)^{3/2}}{2\pi A(x)} \int_{-\infty}^{\infty} dx' \frac{(x+x')[\zeta_1(x) - \zeta_1(x')]}{(x-x')[1 + \frac{1}{4}(x+x')^2]} \cong \sigma. \quad (2.10)$$

In writing (2.10), we have anticipated that σ^* and the associated $\zeta_1(x)$ will vanish at $\alpha=0$ and that, therefore, we can use $d\zeta/dx \cong -x$ in the argument of the anisotropy function A . As in previous work,^{13,14} the terms proportional to σ on the left-hand side of (2.10) have been re-

tained because we expect derivatives with respect to x to produce factors of $\sigma^{-1/2}$. Had we omitted these terms, the remaining singular integral equation for $\zeta_1(x)$ would have determined a smooth shape correction¹⁹ of order σ but not a solvability condition for σ^* .

The mathematical structure of (2.10) seems easiest to study if we eliminate the first derivative on the left-hand side by writing

$$\xi_1(x) = (1+x^2)^{3/4} Z(x). \quad (2.11)$$

The result is

$$(\mathcal{D}_2 + \mathcal{A}_2)Z = \frac{\sigma}{(1+x^2)^{3/4}}, \quad (2.12)$$

where \mathcal{D}_2 is a self-adjoint differential operator:

$$\mathcal{D}_2 = \sigma \frac{d^2}{dx^2} + \frac{(1+x^2)^{1/2}}{A(x)} + O(\sigma) \quad (2.13)$$

and

$$\begin{aligned} \mathcal{A}_2 Z(x) &= \mathcal{P} \int_{-\infty}^{\infty} dx' \mathcal{A}_2(x, x') Z(x') \\ &= \frac{(1+x^2)^{3/4}}{2\pi A(x)} \\ &\quad \times \mathcal{P} \int_{-\infty}^{\infty} dx' \frac{1}{x-x'} \\ &\quad \times \frac{(x+x')[1+(x')^2]^{3/4}}{[1+\frac{1}{4}(x+x')^2]} Z(x'). \end{aligned} \quad (2.14)$$

In (2.13) we have neglected a nonsingular term of order σ . In (2.14), \mathcal{P} denotes a Cauchy principal value that has become necessary because we are evaluating separately the terms containing $\xi_1(x)$ and $\xi_1(x')$ inside the integral in (2.10). Note that, apart from the factor $A^{-1}(x)$, $\mathcal{A}_2(x, x')$ is an antisymmetric kernel.

The solvability condition for (2.12) has the form

$$\Lambda(\sigma, \alpha) \equiv \int_{-\infty}^{\infty} dx \frac{\tilde{Z}^H(x)}{(1+x^2)^{3/4}} = 0, \quad (2.15)$$

where \tilde{Z}^H is a null eigenvector of the adjoint operator $\mathcal{D}_2 + \mathcal{A}_2$:

$$(\mathcal{D}_2 + \tilde{\mathcal{A}}_2) \tilde{Z}^H = 0, \quad (2.16)$$

with $\tilde{\mathcal{A}}_2(x, x') = \mathcal{A}_2(x', x)$.

To solve (2.16), we adopt a strategy that (we believe) was first used by Kessler, Koplik, and Levine.²⁰ Suppose that one solution of (2.16), say \tilde{Z}_+^H , has the WKB form $\exp[S_+(x)/\sqrt{\sigma}]$, where S_+ is some function of x which remains finite and smooth in the limit $\sigma \rightarrow 0$. Further, suppose that $S_+(x)$ has a point of stationary phase \bar{x}_+ in the upper half of the complex x plane, and that integrals like those appearing in (2.14) or (2.15) can be evaluated in the limit of small σ by deforming the contour of integration into the path of steepest descent through \bar{x}_+ . The latter condition requires $\text{Re}S_+(\bar{x}_+) < 0$. Then the only contribution to $\tilde{\mathcal{A}}_2 \tilde{Z}_+^H$ that is not exponentially small of order $\exp[S_+(\bar{x}_+)/\sqrt{\sigma}]$ is the part that comes from integrating around the pole at $x = x'$. In a similar manner, we can define \tilde{Z}_-^H to be that solution of (2.16) for which the appropriate path of steepest descent lies in the lower half-plane, and for which the exponentially accurate approximation to $\tilde{\mathcal{A}}_2 \tilde{Z}_-^H$ is obtained by closing the contour

around $x = x'$ in the opposite sense. In this way, (2.16) becomes

$$\sigma \frac{d^2}{dx^2} \tilde{Z}_\pm^H + \frac{(1+x^2)^{1/2}}{A(x)} (1 \pm ix) \tilde{Z}_\pm^H \cong 0. \quad (2.17)$$

It is now a simple matter to construct the WKB solutions to (2.17):

$$\tilde{Z}_\pm^H(x) \approx \frac{A^{1/4}(x)}{(1+x^2)^{3/8}} (1 \pm ix)^{1/4} \exp \left[\frac{1}{\sqrt{\sigma}} S_\pm(x) \right], \quad (2.18)$$

where

$$S_\pm(x) = \pm i \int_0^x dx' \frac{(1 \pm ix')^{1/4} (1 \pm ix')^{3/4}}{A^{1/2} x'}. \quad (2.19)$$

The points of stationary phase occur at $\bar{x}_\pm = \pm i$ as required. Note that $S_+(x) = S_-^*(x)$ and that $S_+(-x) = S_-(x) = S_+^*(x)$. Thus the \tilde{Z}_\pm^H form a complex-conjugate pair, and the solvability function $\Lambda(\sigma, \alpha)$ is a real number which does not depend upon whether \tilde{Z}^H is chosen to be \tilde{Z}_+^H or \tilde{Z}_-^H in (2.15). In fact, no choice is available to us because the only physically acceptable \tilde{Z}^H is the symmetric combination $\tilde{Z}_+^H + \tilde{Z}_-^H = 2 \text{Re} \tilde{Z}_+^H$. Moreover, for $x \rightarrow \pm \infty$, we find

$$\text{Re} \tilde{Z}_+^H(x) \approx \exp \left[-\frac{x^2}{2(2\sigma)^{1/2}} \right] \cos \left[\frac{x^2}{2(2\sigma)^{1/2}} \right], \quad (2.20)$$

which means that the integration in (2.15) converges rapidly.

There is a mathematical subtlety that deserves mention at this point in the discussion. If we compute the homogeneous solutions Z_\pm^H for the original linear operator $\mathcal{D}_2 + \mathcal{A}_2$ rather than its adjoint, we find that the exponential in (2.20) is divergent at large $|x|$, that is, $-x^2$ is replaced by $+x^2$. The question then arises whether these null eigenvectors Z_\pm^H belong in the original function space in which we are trying to invert $\mathcal{D}_2 + \mathcal{A}_2$ and, if not, whether $\mathcal{D}_2 + \mathcal{A}_2$ might be nonsingular after all. (Just this possibility has been raised, on other grounds, by Van Saarloos and Weeks.²¹) In more specific terms, suppose that we construct a representation of the operator $\mathcal{D}_2 + \mathcal{A}_2$ in a complete set of functions which remain bounded at infinity, truncate this representation at some high order, and then invert the operator to find an approximate solution of (2.12). Might this solution exist for arbitrary values of σ ? We suspect that it would, but that it would not converge uniformly in x as we increase the order of the truncation. Our approximation for $Z(x)$ might look more and more like $Z_\pm^H(x)$ for large x as the ‘‘accuracy’’ is increased—except, of course, for the special cases where $\sigma = \sigma^*$.

We cannot prove this speculation rigorously at present, but we can offer several arguments in its favor. Note that (2.15) is at least a necessary condition for the existence of solutions of (2.12); it can be obtained simply by multiplying (2.12) on the left by \tilde{Z}^H and integrating over x . Thus there seems to be little doubt about the breakdown of the Ivantsov solutions. The real question is whether the solvability condition is sufficient for determining the existence of any solutions whatsoever. There are two pieces

of circumstantial evidence that support sufficiency. First, the solvability principle turns out to be exactly correct for the local models^{13,14} in which many of the above features appear but where the actual solutions of the inhomogeneous equations analogous to (2.12) can be constructed explicitly. Second, the operator inversion suggested in the previous paragraph is not very different in principle from the numerical calculations^{9,10} in which convergence at infinity has been enforced but a cusp has been allowed to occur at $x = 0$. In both of the latter kinds of investigations, selection of special values of $\sigma = \sigma^*$ has been confirmed.

We turn now to an evaluation of the solvability function $\Lambda(\sigma, \alpha)$ defined in (2.15). We consider only the limit of small σ so that integrations can be performed by the method of steepest descent. Look first at the isotropic case, $\alpha = 0$. The situation is mathematically almost identical to what was found in the nearly local limit, $p \rightarrow \infty$.¹ Choose $\tilde{Z}^H = \tilde{Z}_+^H$ in (2.15); then the dominant contribution comes from the neighborhood of $\bar{x}_+ = +i$, where

$$S_+(x) \cong -\bar{a} - \frac{4}{7} \left[\frac{2}{i} \right]^{1/4} (x-i)^{7/4} \tag{2.21}$$

with

$$\bar{a} = \int_0^1 du (1+u)^{1/4} (1-u)^{3/4} \cong 0.6159 \dots \tag{2.22}$$

Performing the integration, we find

$$\Lambda(\sigma, 0) \approx \frac{N}{\sigma^b} \exp \left[-\frac{\bar{a}}{\sqrt{\sigma}} \right], \tag{2.23}$$

where $b = \frac{1}{28}$ and N is a σ -independent constant which is not of any significance in the present context. Equation (2.23), which indicates the absence of needle-crystal solutions at nonzero σ for $\alpha = 0$ and also illustrates the singular nature of the capillary perturbation, seems consistent with the recent numerical results.^{9,10}

For small, positive anisotropy strength α , our analysis is almost identical to one that we have presented recently¹⁴ for the local boundary-layer model at small Δ . Inserting the expression (2.5) for A into (2.19), we find that $S_+(x)$ has a new branch point at $x_b \cong i(1 - \sqrt{2\alpha})$. Let the associated branch cut extend from x_b upward along the imaginary x axis so that the point of stationary phase, which remains at $x = i$, becomes in effect a pair of such points located on either side of this cut. This configuration of singularities is shown in Fig. 1 along with the con-

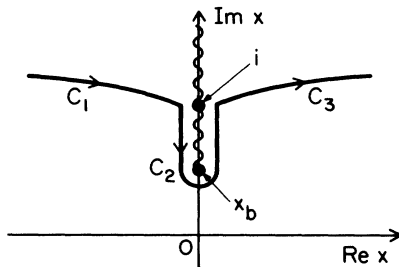


FIG. 1. Path of steepest descent for the evaluation of $\Lambda(\sigma, \alpha)$.

tour of integration whose sections are labeled C_1 , C_2 , and C_3 . In the immediate neighborhood of $x = i$, we find

$$S_+(x) - S_+(i \pm 0) \approx \mp \frac{2\sqrt{2}}{11} \left[\frac{2}{i} \right]^{1/4} \frac{(x-i)^{11/4}}{\sqrt{\alpha}}, \tag{2.24}$$

valid for $|x - i| \ll \sqrt{\alpha} \ll 1$, where the upper and lower signs denote values obtained by approaching the cut from the right and left sides, respectively. For values of σ small enough that $\exp(S_+/\sqrt{\sigma})$ oscillates many times along C_2 and drops off sharply away from the cut along C_1 and C_3 , the steepest-descent estimate for Λ must yield a result of the form

$$\Lambda(\sigma, \alpha) \sim \exp \left[-\frac{\bar{a}}{\sqrt{\sigma}} \right] \cos \left[\frac{1}{\sqrt{\sigma}} \text{Im} S_+(i) \right], \tag{2.25}$$

which oscillates increasingly rapidly as $\sigma \rightarrow 0$. On the other hand, when σ becomes large enough (or α small enough) that $\exp(S_+/\sqrt{\sigma})$ varies only slowly across C_2 , then the oscillations must cease and Λ must revert to smooth behavior characteristic of $\alpha = 0$.

The range of values of σ where the crossover between oscillating and nonoscillating Λ occurs necessarily includes the largest σ which satisfies the solvability condition $\Lambda = 0$; and it is this largest $\sigma = \sigma^*$ that identifies the dynamically selected needle crystal. The infinitely many smaller σ 's for which Λ vanishes all seem to describe unstable solutions of no obvious dynamical significance. Mathematically, this crossover occurs when the magnitude of the right-hand side of (2.24) is of order $\sqrt{\sigma}$ at the branch point x_b where $|x_b - i| \cong \sqrt{2\alpha}$. Thus

$$\sigma^* \approx \sigma_0 \alpha^{7/4}, \tag{2.26}$$

where σ_0 is a number of order unity. The power $\frac{7}{4}$ is somewhat larger than recent numerical estimates; further tests of this prediction would be valuable.

For completeness, let us summarize the above results by writing out, in dimensional form, the selection laws for velocity v and tip radius ρ for the two-dimensional symmetric model in the limit of small undercooling Δ . From (2.6), we have $p \approx (\Delta/\pi)^2$. Then, combining definitions of p and σ , we have

$$v \approx \left[\frac{2D}{\bar{d}_0} \right] \sigma^* p^2 \approx \sigma^* \left[\frac{2D}{\bar{d}_0} \right] \frac{\Delta^4}{\pi^2} \tag{2.27}$$

and

$$\rho \approx \frac{\bar{d}_0}{\sigma^* p} \approx \frac{\bar{d}_0}{\sigma^*} \frac{\pi}{\Delta^2}. \tag{2.28}$$

So far as we know, there exists no experimental data against which to check these predictions. It seems not inconceivable that relevant experiments could be carried out using sufficiently thin samples to achieve effective two-dimensionality. The strong dependence on undercooling and the strength of the anisotropy would be specially interesting to verify.

III. THREE DIMENSIONS

The analog of (2.1) for a three-dimensional needle crystal described in cylindrical coordinates by $z = \zeta(r, \phi)$ is

$$\Gamma_3\{p, r, \zeta(r, \phi)\} = \int_0^\infty d\tau \frac{1}{(2\pi\tau)^{3/2}} \int_0^\infty dr' r' \int_0^{2\pi} d\phi' \exp \left\{ -\frac{p}{2\tau} \{r^2 + (r')^2 - 2rr' \cos(\phi - \phi') + [\zeta(r, \phi) - \zeta(r', \phi') + \tau]^2\} \right\} \quad (3.2)$$

and

$$\mathcal{X}_3\{\zeta\} = -\nabla \cdot \left[\frac{\nabla \zeta}{[1 + (\nabla \zeta)^2]^{1/2}} \right]. \quad (3.3)$$

Growth is in the z direction; points in a plane perpendicular to the z axis are located by the polar coordinates r, ϕ ; and ∇ denotes a two-dimensional gradient in this plane. In the case of vanishing surface tension, (3.1) admits a continuous family of axisymmetric Ivantsov solutions

$$\zeta_{Iv}(r) = -r^2/2, \quad (3.4)$$

with

$$\sigma \frac{d^2 \zeta_1}{dr^2} + \frac{\sigma(1-2r^2)}{r(1+r^2)} \frac{d\zeta_1}{dr} + \frac{(1+r^2)^{3/2}}{4\pi} \int_0^\infty dr' r' \int_0^{2\pi} d\phi' \frac{[(r')^2 - r^2][\zeta_1(r) - \zeta_1(r')]}{\{r^2 + (r')^2 - 2rr' \cos\phi' + \frac{1}{4}[r^2 - (r')^2]^2\}^{3/2}} \cong \sigma(2+r^2). \quad (3.6)$$

Once again, the single remaining parameter, $\sigma = 2d_0D/v\rho^2$, is the coefficient of the highest derivatives in an inhomogeneous linear equation and, once again, we expect that this equation will have physically acceptable solutions—if it has any at all—only for special values of this parameter.

The next step is to perform the integration over the angle ϕ' . Define the quantity

$$\beta(r, r') \equiv \frac{r^2 + (r')^2 + \frac{1}{4}[r^2 - (r')^2]^2}{2rr'} \quad (3.7)$$

and the elliptic integral

$$J(\beta) \equiv \int_0^{2\pi} d\phi \frac{1}{(\beta - \cos\phi)^{3/2}}. \quad (3.8)$$

Then the integral in (3.6) becomes

$$\frac{(1+r^2)^{3/2}}{4\pi} \int_0^\infty dr' r' \frac{[(r')^2 - r^2]}{(2rr')^{3/2}} J(\beta(r, r')) \times [\zeta_1(r) - \zeta_1(r')]. \quad (3.9)$$

Note that

$$\beta - 1 = \frac{(r - r')^2 [1 + \frac{1}{4}(r + r')^2]}{2rr'}. \quad (3.10)$$

Our experience in two dimensions leads us to anticipate that the dominant contribution to (3.9) will come from the neighborhood of the singularity in J at $r = r', \beta = 1$:

$$J(\beta) \cong \frac{2\sqrt{2}}{\beta - 1} + (0.1716\dots) \ln(\beta - 1) + \dots \quad (3.11)$$

$$\Delta - \frac{d_0}{\rho} \mathcal{X}_3\{\zeta(r, \phi)\} = p^{3/2} \Gamma_3\{p, r, \zeta(r, \phi)\}, \quad (3.1)$$

where

$$\Delta = p \Gamma_3\{p, r, \zeta_{Iv}(r)\} = pe^p \int_p^\infty dy \frac{e^{-y}}{y} \approx -p \ln p, \quad (3.5)$$

where the last approximation is valid for small p . (In fact, there exists a more general class of paraboloidal solutions with elliptical cross sections.²²)

We now repeat the steps that led to (2.10): Subtract (3.5) from (3.1), divide by p , linearize in $\zeta_1 = \zeta - \zeta_{Iv}$, and take the limit $p \rightarrow 0$. At present, we have completed calculations only for the situation in which the surface tension is isotropic so that ζ_1 is a function of r only. The result is

If we keep just the leading term in (3.11), then (3.9) becomes

$$\frac{(1+r^2)^{3/2}}{2\pi} \int_0^\infty dr' \left[\frac{r'}{r} \right]^{1/2} \frac{(r'+r)[\zeta_1(r) - \zeta_1(r')]}{(r'-r)[1 + \frac{1}{4}(r+r')^2]}, \quad (3.12)$$

which looks similar in many respects to the integral in (2.10).

There are, however, some important differences between (2.10) and (3.12). The integration in (3.12) starts at $r' = 0$ instead of at $-\infty$, and there is no symmetry that might allow us to extend the integration to the infinite interval. There is even a branch point at $r' = 0$. As a result, the path of steepest descent into which we shall bend this contour of integration will not be so simple as it was in two dimensions, and the accuracy of the approximation will be algebraic in σ rather than exponential. A related complication is caused by the logarithm in (3.11).

Continuing to follow the strategy that we used in two dimensions, we symmetrize the differential operator in (3.6) by writing

$$\zeta_1(r) = \frac{(1+r^2)^{3/4}}{\sqrt{r}} W(r) \quad (3.13)$$

so that the full equation takes the form

$$(\mathcal{D}_3 + \mathcal{A}_3)W = \frac{\sigma\sqrt{r}(2+r^2)}{(1+r^2)^{3/4}}. \quad (3.14)$$

Here \mathcal{D}_3 is the differential operator:

$$\mathcal{D}_3 = \sigma \left[\frac{d^2}{dr^2} + \frac{1}{4r^2} \right] + Q_1(r) + O(\sigma), \quad (3.15)$$

where

$$Q_1(r) = \frac{(1+r^2)^{3/2}}{2\pi^{3/2}} \int ds \sqrt{s} \int d\mathbf{r} [(r')^2 - r^2] \exp(-s \{ |\mathbf{r} - \mathbf{r}'|^2 + \frac{1}{4}[r^2 - (r')^2]^2 \})$$

and then make a series of transformations essentially the same as those used by Pelcé and Pomeau² for deriving the Ivantsov formula.] Notice the term $\sigma/4r^2$ that has been kept in (3.15) because it diverges at $r=0$. \mathcal{A}_3 is an antisymmetric singular integral operator:

$$\begin{aligned} \mathcal{A}_3 W &\equiv \mathcal{P} \int_0^\infty dr' \mathcal{A}_3(r, r') W(r') \\ &= \frac{1}{8\pi\sqrt{2}} \mathcal{P} \int_0^\infty dr' (1+r^2)^{3/4} \frac{[r^2 - (r')^2]}{rr'} \\ &\quad \times [1 + (r')^2]^{3/4} J(\beta(r, r')) W(r'). \end{aligned} \quad (3.17)$$

To construct the solvability condition for (3.14), we must compute the adjoint null eigenfunctions \tilde{W}_\pm^H which satisfy

$$(\mathcal{D}_3 - \mathcal{A}_3) \tilde{W}_\pm^H = 0. \quad (3.18)$$

As before, we expect these functions to have the WKB form, say, $\exp[R_\pm(r)/\sqrt{\sigma}]$, where the $R_\pm(r)$ have points of stationary phase $\bar{r}_\pm = \pm i$ in the upper (lower) half of the complex r plane such that $\text{Re}R_\pm(\bar{r}_\pm) < 0$. (The points of stationary phase always turn out to be at $\pm i$ because the analytic continuation of the Ivantsov solution diverges at those points.) The contour appropriate for evaluating the integral $\mathcal{A}_3 \tilde{W}_\pm^H$ is shown in Fig. 2. Strictly speaking, what is shown here is a deformation of the part of the principal-value integration that originally ran along the

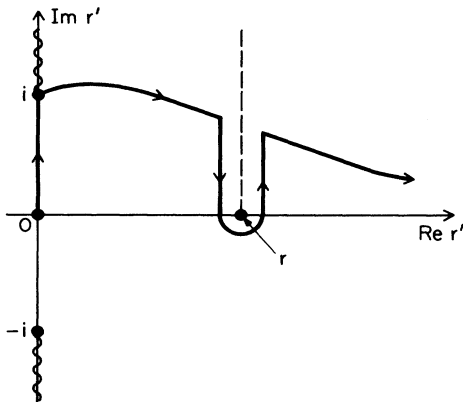


FIG. 2. Contour for evaluation of $\mathcal{A}_3 \tilde{W}_\pm^H$ in Eq. (3.17).

$$\begin{aligned} Q_1(r) &= \frac{(1+r^2)^{3/2}}{4\pi} \mathcal{P} \int_0^\infty dr' r' \frac{[(r')^2 - r^2]}{(2rr')^{3/2}} J[\beta(r, r')] \\ &= (1+r^2)^{1/2}. \end{aligned} \quad (3.16)$$

[To obtain the final, surprisingly simple—but exact—expression for Q_1 , write it in the form

positive real axis and passed below the singularity at $r'=r$. The wiggly lines along the imaginary axis indicate cuts associated with branch points at $\pm i$; and the dashed line is a cut associated with the logarithm in (3.11).

All portions of this contour which lie above the real axis make exponentially small contributions to this integral. Along the path from the origin to $\bar{r}_+ = i$, the integrand will turn out to be proportional to $\exp(-|r'|/\sqrt{\sigma})$ multiplied by some power of $|r'|$; thus this contribution to the integral will vanish like some power of σ and, because it is not the coefficient of a differential operator in (3.18), must be neglected. A similar argument tells us to neglect the contribution from the discontinuity across the logarithmic branch cut. We are left, therefore, with only the contribution from the pole at $r=r'$, which we can compute directly from (3.12). Generalizing to account for the \pm options, we find

$$\mathcal{A}_3 \tilde{W}_\pm^H \approx \mp ir (1+r^2)^{1/2} \tilde{W}_\pm^H. \quad (3.19)$$

The remarkable result of the above analysis is that (3.18) has almost the same form as (2.17):

$$\sigma \left[\frac{d^2}{dr^2} + \frac{1}{4r^2} \right] \tilde{W}_\pm^H + (1+r^2)^{1/2} (1 \pm ir) \tilde{W}_\pm^H \cong 0. \quad (3.20)$$

For $r \gg \sqrt{\sigma}$, we can compute the WKB solutions as before:

$$\tilde{W}_\pm^H(r) \approx \frac{(1 \mp ir)^{1/4}}{(1+r^2)^{3/8}} \exp \left[\frac{1}{\sqrt{\sigma}} R_\pm(r) \right] \quad (3.21)$$

with

$$R_\pm(r) = \pm i \int_0^r dr' (1 \mp ir')^{1/4} (1 \pm ir')^{3/4}. \quad (3.22)$$

For $r \ll 1$, however, (3.20) has only one solution that is regular at $r=0$:

$$\tilde{W}^H(r) \cong \sqrt{r} J_0(r/\sqrt{\sigma}) \approx \cos \left[\frac{r}{\sqrt{\sigma}} - \frac{\pi}{4} \right], \quad (3.23)$$

where J_0 is a Bessel function and the last approximation is valid for $r \gg \sqrt{\sigma}$. We therefore match (3.21) and (3.23) in the region $\sqrt{\sigma} \ll r \ll 1$ to obtain the appropriate null eigenvector:

$$\tilde{W}^H = \tilde{W}_+^H e^{-i\pi/4} + \tilde{W}_-^H e^{i\pi/4}. \quad (3.24)$$

This is the analog of the choice of the symmetric combination of the \tilde{Z}_\pm^H in two dimensions. Here, in the

three-dimensional problem, the boundary condition at $r=0$ seems to be playing a specially important role. We can now write the solvability condition explicitly:

$$\Pi(\sigma) \equiv \text{Re} \int_0^\infty dr \sqrt{r} \frac{(2+r^2)(1-ir)^{1/4}}{(1+r^2)^{9/8}} \times \exp \left[\frac{1}{\sqrt{\sigma}} R_+(r) - \frac{i\pi}{4} \right] = 0. \quad (3.25)$$

The path of steepest descent for evaluation of $\Pi(\sigma)$ is the same as that shown in Fig. 2 except that the excursion back to the real axis and around the singularity at $r=r'$ is missing. Now a remarkable cancellation occurs; the integrand in (3.25) for imaginary r is purely imaginary, thus the integration from $r=0$ to $r=i$ makes no contribution to Π . Apart from an uninteresting constant prefactor, the three-dimensional $\Pi(\sigma)$ has reverted to the two-dimensional $\Lambda(\sigma)$ given in (2.23). (The same thing happens in the limit $p \rightarrow \infty$.¹)

The above result presents an interesting puzzle because experimental evidence in three dimensions indicates little, if any, dependence of the dendritic growth rate on the strength of the crystalline anisotropy.²³ Addition of a purely axisymmetric anisotropy to the calculation presented here would produce a σ^* of the form (2.26), which

would seem to be unacceptable. There are many possible explanations for the apparent discrepancy. The experiments might not be probing the small- α limit implied in (2.26); the difference between the thermal conductivities of the liquid and solid might turn out to be relevant; a kinetic attachment coefficient or a temperature-dependent surface tension might play some role. It is possible, of course, that the solvability mechanism breaks down entirely in three dimensions; the regular perturbation expansion for the shape correction in powers of σ might cease to exist at some finite order, or an axial anisotropy might completely change the structure of the theory. In view of the history of surprises in this subject, it certainly seems possible that we are still missing some fundamental principles.

ACKNOWLEDGMENTS

The authors wish to thank C. Caroli for pointing out to us serious errors in Ref. 8 and in an earlier version of this paper. This research was supported by U.S. Department of Energy Grant No. DE-FG03-84ER45108 and by National Science Foundation Grant No. PHY-82-17853, supplemented by funds from the U.S. National Aeronautics and Space Administration.

¹B. Caroli, C. Caroli, B. Roulet, and J. S. Langer, Phys. Rev. A **33**, 442 (1986); B. Caroli, C. Caroli, C. Misbah, and B. Roulet (unpublished).

²P. Pelcé and Y. Pomeau (to be published).

³M. Ben Amar and Y. Pomeau (unpublished).

⁴J. S. Langer, Rev. Mod. Phys. **52**, 1 (1980).

⁵P. G. Saffman and G. I. Taylor, Proc. R. Soc. London, Ser. A **245**, 312 (1958).

⁶B. I. Shraiman, Phys. Rev. Lett. **56**, 2028 (1986).

⁷R. Combescot, T. Dombre, V. Hakim, Y. Pomeau, and A. Pumir, Phys. Rev. Lett. **56**, 2036 (1986).

⁸D. C. Hong and J. S. Langer, Phys. Rev. Lett. **56**, 2032 (1986).

Although the results obtained in this paper agree with those of Refs. 6 and 7 and apparently are correct, the presentation is, at best, misleading. Equation (16) is not an exact solution of the inhomogeneous singular integral equation (5). A more satisfactory derivation of the solvability condition (20) can be constructed using the methods described in the present paper, which are essentially those discussed by Shraiman in Ref. 6.

⁹D. Meiron, Phys. Rev. A **33**, 2704 (1986).

¹⁰D. Kessler and H. Levine, Phys. Rev. A **33**, 7867 (1986).

¹¹R. Brower, D. Kessler, J. Koplik, and H. Levine, Phys. Rev. Lett. **51**, 1111 (1983); Phys. Rev. A **29**, 1335 (1984); D. Kessler, J. Koplik, and H. Levine, *ibid.* **30**, 3161 (1984); **31**, 1712 (1985).

¹²E. Ben-Jacob, N. Goldenfeld, J. S. Langer, and G. Schon, Phys. Rev. Lett. **51**, 1930 (1983); Phys. Rev. A **29**, 330 (1984);

E. Ben-Jacob, N. Goldenfeld, B. G. Kotliar, and J. S. Langer, Phys. Rev. Lett. **53**, 2110 (1984).

¹³J. S. Langer, Phys. Rev. A **33**, 435 (1986).

¹⁴J. S. Langer and D. C. Hong, Phys. Rev. A **34**, 1462 (1986).

¹⁵M. Kruskal and H. Segur (unpublished). Some discussion of these techniques appears in Refs. 3, 7, and 14.

¹⁶G. P. Ivantsov, Dokl. Akad. Nauk SSSR **58**, 567 (1947).

¹⁷M. E. Glicksman, R. J. Shaefer, and J. D. Ayers, Metall. Trans. A **7**, 1747 (1976); S. C. Huang and M. E. Glicksman, Acta Metall. **29**, 701 (1981); **29**, 717 (1981).

¹⁸J. S. Langer and H. Müller-Krumbhaar, Acta Metall. **26**, 1681 (1978); **26**, 1689 (1978); **26**, 1697 (1978).

¹⁹An exact expression for the first-order shape correction appears in the Appendix to H. Müller-Krumbhaar and J. S. Langer, Acta Metall. **26**, 1697 (1978). A typographical error in the final formula, Eq. (A.10), is corrected in H. Müller-Krumbhaar and J. S. Langer, Acta Metall. **29**, 145 (1981), Eq. (2.39).

²⁰D. Kessler, J. Koplik, and H. Levine, in Proceedings of the NATO Advanced Research Workshop on Patterns, Defects, and Microstructures in Non-Equilibrium Systems, Austin, Texas, March, 1986 (unpublished).

²¹W. Van Saarloos and J. Weeks, Phys. Rev. Lett. **55**, 1685 (1985).

²²G. Horvay and J. W. Cahn, Acta Metall. **9**, 695 (1961).

²³M. E. Glicksman (private communication).